

Numerical study of anomaly detection under rail track using a time-variant moving train load

Song-Hun Chong¹, Gye-Chun Cho^{*1}, Eun-Soo Hong¹ and Seong-Won Lee²

¹ Department of Civil Engineering, Korean Advanced Institute for Science and Technology, 291 Daehak-ro, Yuseong-gu, Daejeon 34141, Republic of Korea

² Geotechnical Engineering Research Institute, Korea Institute of Civil Engineering & Building Technology, 283, Goyang-daero, Ilsanseo-gu, Goyang-si, Gyeonggi-do, 10223, Republic of Korea

(Received June 21, 2016, Revised April 03, 2017, Accepted April 13, 2017)

Abstract. The underlying ground state of a railway plays a significant role in maintaining the integrity of the overlying concrete slab and ultimately supporting the train load. While effective nondestructive tests have been used to evaluate the rail track system, they can only be performed during non-operating time due to the stress wave generated by active sources. In this study, finite element numerical simulations are conducted to investigate the feasibility of detecting unfavorable substructure conditions by using a moving train load. First, a train load module is developed by converting the train load into time-variant equivalent forces. The moving forces based on the shape functions are applied at the nodes. A parametric study that takes into account the bonding state and the train class is then performed. All the synthetic signals obtained from numerical simulations are analyzed at the frequency domain using a Fast Fourier transform (FFT) and at the time-frequency domain using a Short-Time Fourier transform (STFT). The presence of a void condition amplifies the acceleration amplitude and the vibration response. This study confirms the feasibility of using a moving train load to systematically evaluate a rail track system.

Keywords: underlying ground states of railway; train load module; fourier transform; short-time fourier transform; finite element numerical simulations

1. Introduction

Rail track is a fundamental component of railway infrastructure. In particular, underlying ground states of a railway play a significant role in maintaining the integrity of the overlying concrete slab and ultimately supporting the train load. Thus, reliable and effective evaluation of the ground states is a critical issue for safe and secure train operation. The damage pattern of a railway structure system can be classified as follows: (1) crack initiation and crack growth of the slab track; (2) settlement of the railway embankment; (3) subsoil deformation induced by excavation of an existing railway tunnel. Any of these damages may cause severe instability problems and malfunctions of railway systems.

Core samples taken from the concrete slab of railway system can be used to investigate the quality of the concrete slab and the bonding state between slab and subsoil. However, these conditions may not be reliably estimated with the extracted samples because the coring process

*Corresponding author, Professor, E-mail: gyechun@kaist.edu

can disturb in situ conditions and cause structural damage. As an alternative approach, the integrity of a railway system can be evaluated by employing a nondestructive inspection methods such as an impact-based method (De Chiara *et al.* 2012), ground penetrating radar (Hugenschmidt 2000), or acoustic emission (Luo *et al.* 2004). In particular, the impact-based method is potentially optimal for this application because it simply uses the reflected time waveform of vibration resonance induced by an impact source. The signal obtained by the displacement response of the receiver can be analyzed in the time and frequency domains (ASTM C 1383). Many studies have widely used the conventional impact method to investigate the void size, flaw depth, and plate thickness in concrete structures (Carino and Sansalone 1990, Lin *et al.* 1990, 1991, Carino 2013). Recently, this method coupled with Fourier transform and short-time Fourier transform has been applied to evaluate the bonding state of tunnel shotcrete (Song and Cho 2009, 2010). Compared to other applications, the rail track system has an inherent limitation with respect to applying the conventional impact-based method due to the train operating schedule. Instead of using an active source, the train load can be used to generate a stress wave into the railway and obtain the signal from installed sensors. For example, geophones attached to sleepers can record the displacements of track during the loading event. The use of dynamic loading from scheduled trains overcomes the difference in the response observed between static and dynamic loading and allows the quantification of the track modulus (Priest and Powrie 2009). The numerical analysis of ballasted rail track shows that the relative stiffness difference among substructure components has pronounced on the track dynamic interaction (Cai and Raymond 1994, Mosayebia *et al.* 2017). In particular, the vibration response on rail track is significantly affected by the critical speed relevant to relation by between the train speed and the wave velocity of the subgrade (Dawn 1983, Krylov 1995). If the train speed exists above the critical speed, train moving loads produces excessive ground movement on the track structure and increase the risk of train derailling and track structure damage (Madshus and Kaynia 2000, Bian *et al.* 2015, 2016, Sun *et al.* 2016). The numerical simulation presents that the induced wave fronts above the critical speed resembles a plough-shaped response following the loads (Hall 2003). Note that train speed used in this study is fixed at the operating speed (~ 80 km/hr) and the railway responses to a moving load are under quasi-static states. Finite element numerical simulations are conducted to investigate the feasibility of detecting unfavorable substructure conditions under rail track by using a time-variant moving train load. All the signals obtained from numerical simulations are analyzed in the frequency domain using a Fast Fourier transform (FFT) and in the time-frequency domain using a Short-Time Fourier transform (STFT). Emphasis is placed on the use of train loads to automatically evaluate the rail track during long-term operation of railways.

2. Post-processing technique: Shor-time fourier transform

The discrete signal measured in the time domain can be analyzed in the frequency domain using a Fourier transform. However, the frequency domain analysis hinders understanding the time information. A Short-Time Fourier Transform (STFT) can contain both time and frequency information. The discrete time domain signal x is obtained and multiplied by a sliding time window w . The time signal is decomposed into a finite series of sinusoids functions expressed as complex exponentials. The overlapped signal with the sliding window is selected to reduce artificial error at the boundary between two consecutive signals. Sequentially, the Fourier Transform adds a time dimension and a time-varying frequency analysis. The STFT technique

requires proper selection of the time window width and the overlapping size. In particular, the window width in the time domain affects the frequency and time resolutions; a narrow window in the time domain improves the time resolution but decreases the frequency resolution (Santamarina and Fratta 2005). In this study, 512 discrete time signal data points are obtained from a numerical simulation and are divided into 16 sections of equal length with 32 window points (50% overlap between sections).

3. Preliminary numerical simulation: Active impact source

3.1 Preliminary simulation

Generally, the numerical simulation of stress wave propagation is affected by spatial and temporal discretization. Conventional Impact-Echo is simulated to optimize the mesh size and the time increment for numerical stability. The finite element program ABAQUS is used in this study (ABAQUS 2011). Complementary overview of vehicle and ground wave modelling refers to Kouroussis *et al.* (2014). Fig. 1 shows the finite element mesh generated in the preliminary simulation using an active impact source. The railway track is composed of a concrete slab, an

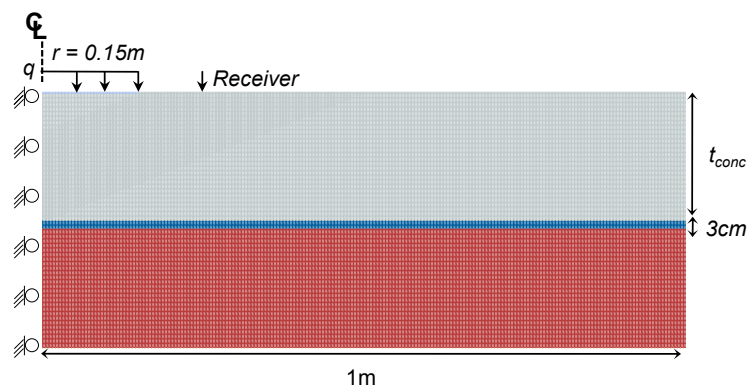


Fig. 1 Finite element mesh generated in the preliminary numerical simulation using an active impact source. Infinite boundary conditions are adopted to absorb the stress wave at the sides. The void condition is simulated by assigning null values to interface elements. t_{con} indicates the concrete thickness

Table 1 Material properties used in this study (Kouroussis *et al.* 2013b)

	Ra il	Railpad	Concrete slab	Hard rock
Density ρ [kg/m ³]	-	-	2400	2600
Young's modulus E_{max} [GPa]	2	-	35	47
Spring stiffness [MN/m]	-	100	-	-
Poisson's ratio ν []	0.3	-	0.2	0.2
P-wave V_p [m/s]	-	-	4000	4500
S-wave V_s [m/s]	-	-	2450	2600
Stiffness-proportional Rayleigh damping coefficient βR []	-	-	1.0E-5	5.0E-7

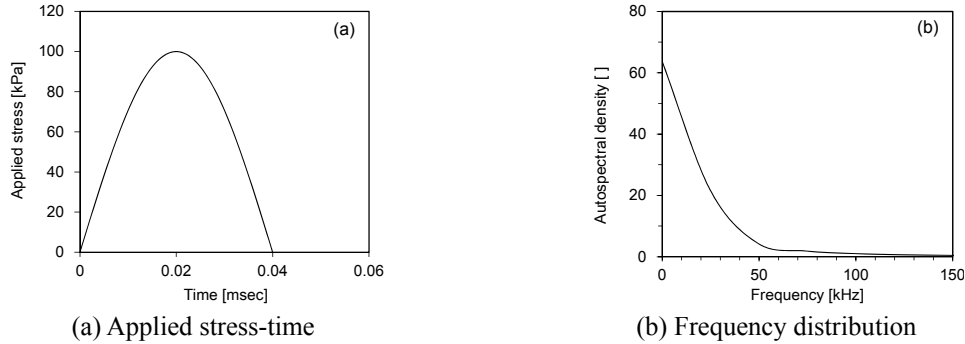


Fig. 2 Applied stress on the surface

underlying hard rock, and a void between these materials. Material properties are tabulated in Table 1. Axisymmetric conditions are modeled with four-node quadrilateral elements.

The receiver is located 0.25 m away from the center of the symmetric axis. The thickness of the concrete slab is 20 cm and the thickness of hard rock base is 60 cm. Infinite elements are adopted to absorb the propagated stress waves at the right side and the bottom. The void condition is modeled by assigning an empty mesh with 3cm thickness. A stress wave is generated by applying the impact source on the surface (Fig. 2). The applied stress-time function is a half sine curve that resembles a typical contact force.

3.2 Results

Fig. 3 presents the results of the time domain waveform, frequency domain, and time-frequency domain obtained from STFT. For the fully bonded condition (Fig. 3(a)), most energy induced by the impact source transmits through the hard rock and the stress wave reflects negligibly from the interface. This causes unclear vibration resonance of the system in frequency domain. The ambiguous resonance is confirmed in the time-frequency analysis, which presents a longer tail along the frequency axis with 0.5 ms resonance duration. Meanwhile, the void condition hinders transmission of the stress wave through the hard rock and the stress wave is completely reflected from the top boundary of void due to the impedance mismatch (Fig. 3(b)). The entrapped energy in the concrete slab causes a typical exponential decay in the time domain and a distinct resonance frequency in the frequency domain. In the time-frequency domain, a longer tail is formed along the time axis: the resonance frequency is 9.5 kHz and its duration is 1.2 ms. From the detected signal, the thickness of the concrete slab t_{con} can be back-calculated with the guided wave theory (Gibson and Popovics 2005)

$$t_{con} = \frac{\alpha \cdot V_p}{\chi \cdot f} \quad (1)$$

where α is a shape factor depending on Poisson's ratio of concrete and χ is an impedance mismatch factor related to the wavelength. For given conditions ($\alpha = 0.953$, $\chi = 2$, $V_p = 4000$ m/s), the estimated t_{con} matches well with the initial geometry of tcon: The $t_{con} = 60$ cm case (not presented here) also provides a good comparison with the obtained $f = 3.2$ kHz. Thus, the preliminary analysis confirms the numerical stability.

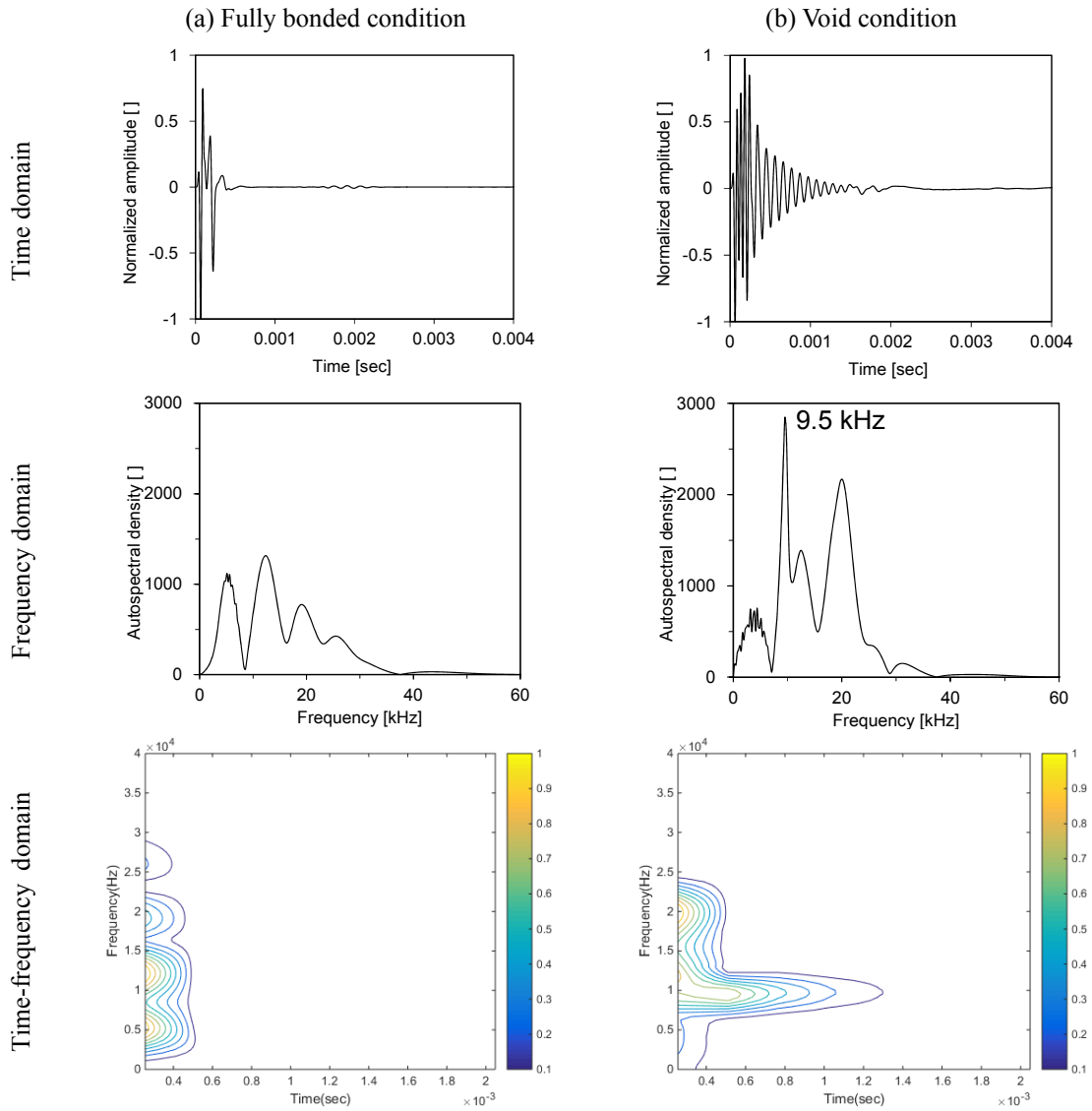


Fig. 3 Time, frequency, and time-frequency domain analyses. An active impact source is applied on the surface. t_{conc} is 20 cm

4. Evaluation of rail track using a moving train load

4.1 Moving load implementation

The dynamic response of civil structures (e.g., bridges and rail track) can be analyzed by using time-variant moving loads technique (Hino *et al.* 1984, Michaltsos *et al.* 1996, Wu *et al.* 2000). The basic concept is to apply time-varying nodal forces on a whole structure, which eventually exerts an equivalent load to point forces that move around the structure. The procedure to implement time-variant moving loads is as follows:

- (1) Select the train class (Table 2) and distance ds between two consecutive sleepers.
- (2) Calculate the time dt when a concentrated force moves with velocity V along the next beam node.
- (3) Obtain a force vector by multiplying the shape functions and train load. Also, the corresponding time vector is obtained by using shape functions and dt .
- (4) Construct a force-time function at a node (Fig. 4(a)). Note that dt_a and dt_c can be used to check the wheel distances a and c .
- (5) Build a set of force-time functions of other nodes by delaying the traveling time.

With respect to the characteristics of the moving load, Fig. 4(b) shows that nodes near to the point where the train travels the train have more concentrated loads whereas nodes far from the concentrated loads have no forces. Note that Hermite's cubic shape functions are used to define the force vector (Hino *et al.* 1984). Fig. 5 shows the finite element mesh to simulate the transient stress variations generated by a moving-load. The rail track system is modeled with a plane strain condition: The rail (a beam) is placed on a railpad with a spring-damper system in the vertical direction. The sleeper below the beam element is placed on the concrete slab. Track properties used for ABAQUS modelling are tabulated in Table 1.

Table 2 Wheel load and base (KRR1 2006)

Train	Total weight [kN]	Wheel load [kN]	Number of axles	Distance between wheels [m]		
				a	b	c
3000	667	83	4	2.4	-	5.2
5000	1246	104	6	2.1	2.1	6.5

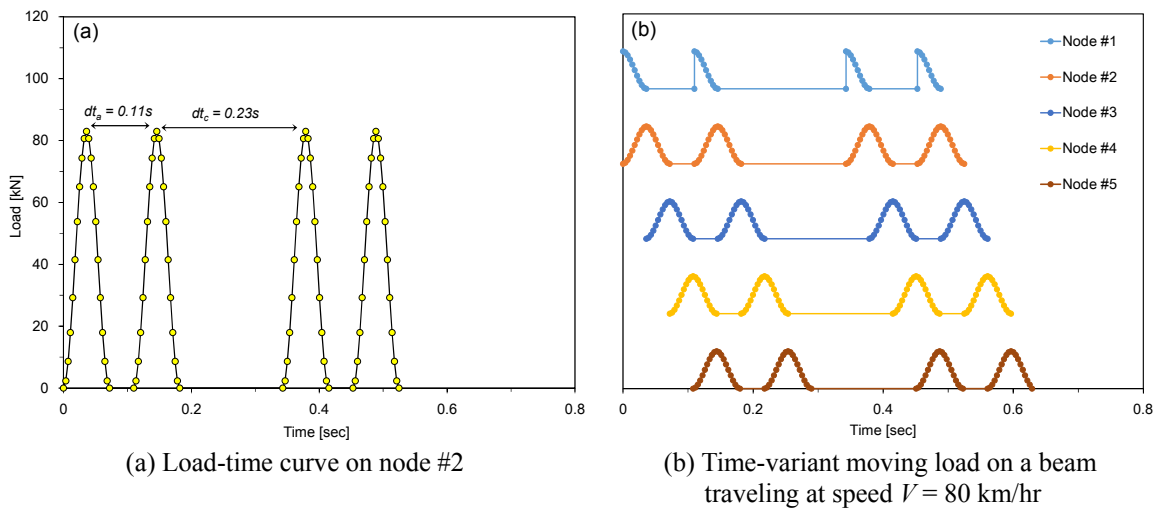
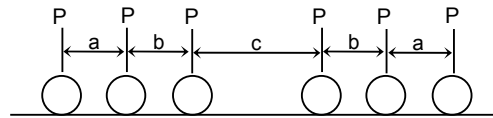


Fig. 4 Description of the moving load that is applied at the beam nodes (Train 3000 class)

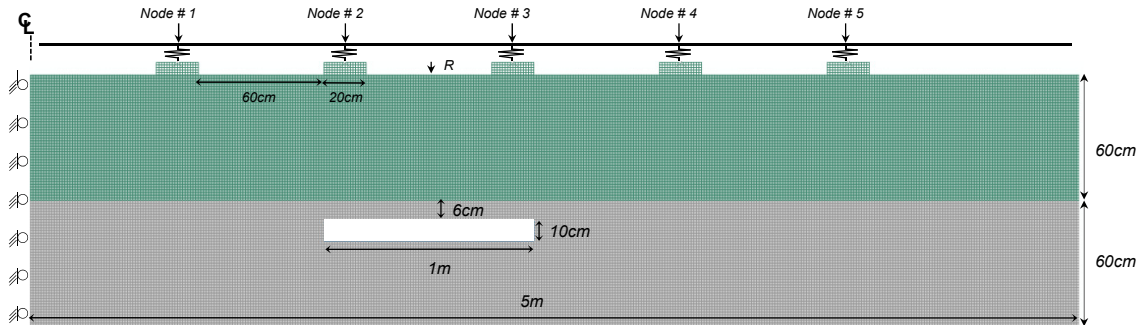


Fig. 5 Finite element mesh to implement the moving load applied at the beam nodes. The reviver *R* is located above the void

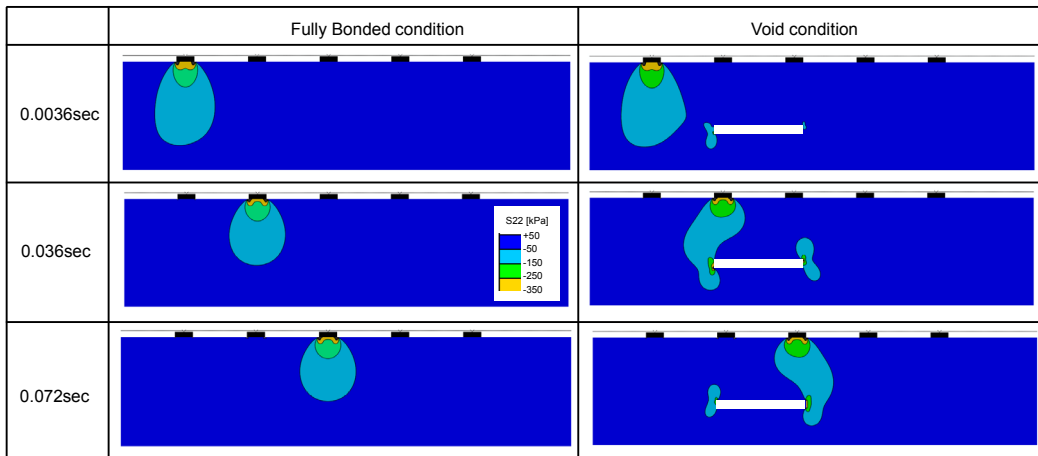


Fig. 6 Stress fields while a 3000 train class travels along the beam at $V = 80$ km/hr

4.2 Results

Fig. 6 presents stress fields induced by the applied concentrated load traveling along the beam node. The absence of a void condition exhibits a general stress distribution below the sleeper at the time, which validates the implementation of moving load. The void condition interacts with the sleeper, and consequently the stress wave is reflected around the void.

The fully bonded and void condition states are simulated with two train classes. It should be noted that the ground vibration mainly depends on the train class (i.e., forcing time during the sleeper passage), and the peak vibration occurs with the critical train speed. However, this study investigates the feasibility of using moving load to evaluate a rail track system, and thus the train speed is fixed at the operating speed (80 km/hr). The results are presented in Figs. 7 and 8. The time domain waveforms show the number of peak accelerations associated with the train class and the moving time along the beam nodes. Compared to the fully bonded state, the presence of a void condition amplifies the acceleration and vibration response. The STFT analysis highlights that the void condition increases the energy density and the contour shape is stretched parallel to the frequency axis at around 120 Hz. This is because the stress wave induced by a moving train load

scarcely transmits around the interface and the reflected wave is entrapped in the concrete slab. An oscillating point load on the surface causes body (P - and S -) and surface (Rayleigh) waves. The energy partition is typically 67% for a R -wave, 26% for a S -wave, and 7% for a P -wave. The surface waves prevail in this type of train-induced analysis, and thus the frequency range is located within a low level, as shown in this study (Kouroussis *et al.* 2013a, 2014). While the use of train load seems to be feasible for the detection of unfavorable substructure conditions, the results show that the differences are quite small and more pronounced at higher frequencies. This low

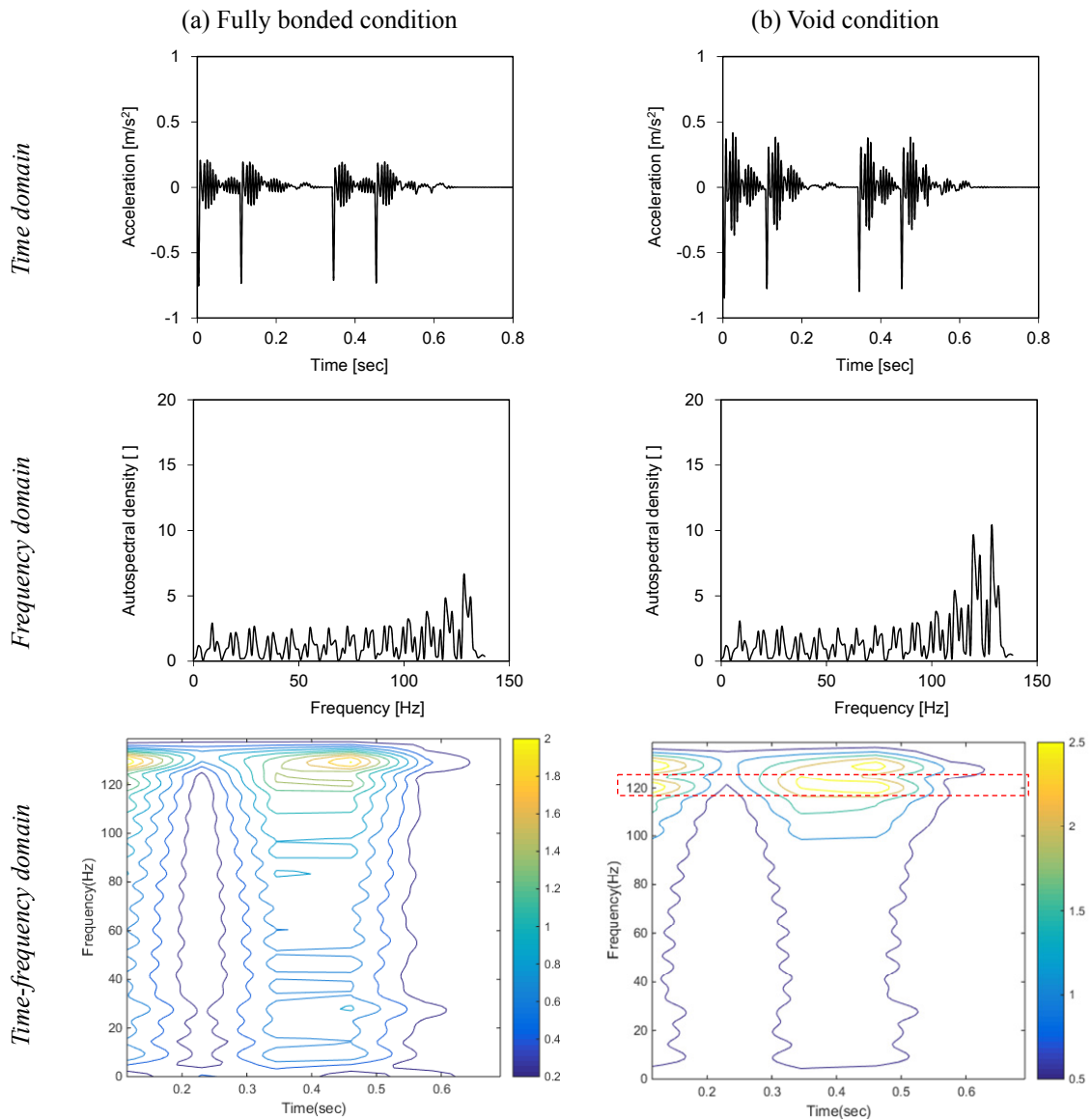


Fig. 7 Time, frequency, and time-frequency domain analyses. A train 3000 class load with 4 wheels is applied along the beam node. In the time-frequency domain, the dotted red square in the void condition indicates the reflected stress wave

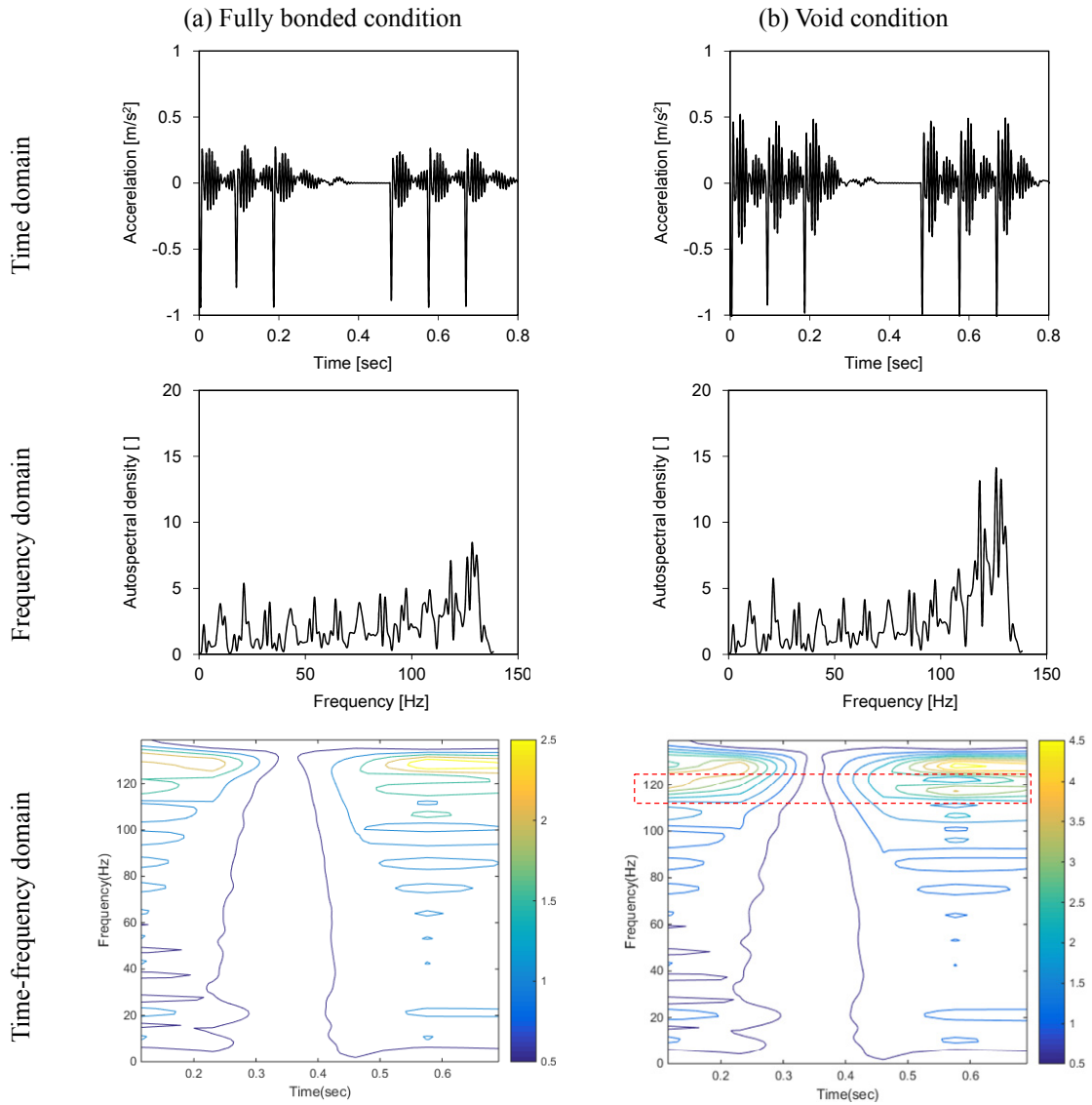


Fig. 8 Time, frequency, and time-frequency domain analyses. A train 5000 class load with 6 wheels is applied along the beam node. In the time-frequency domain, the dotted red square in the void condition indicates the reflected stress wave

scattering efficiency is because the defect size is much smaller than the wavelength in the frequency range used in the simulations. The scattered power has a simple power function of a/λ where the wavelength λ in the medium and the defect size a . In the present analysis wavelength is ~ 20 m at 120 Hz and then a/λ is 0.05. This indicates that the scattered power is very small. However, the dynamic response observed in this study would be more pronounced in the soft soil that has lower wave speeds (and thus higher a/λ), and consequently the vibration response should be stronger and it should be easier to detect a defect under rail track.

5. Conclusions

The damage of railway structure may cause severe instability problems and malfunction of the railway system. While effective nondestructive methods have been used to evaluate it, they can only be performed during non-operating times. The use of train load is potentially optimal for this application because it facilitates generation of stress wave into the railway and automatic signal detections from the installed sensors. In this study, finite element numerical simulations are conducted to investigate the feasibility of detecting unfavorable underground void by using a moving train load. The following conclusions can be drawn:

- Conventional Impact-Echo simulation shows that the void condition hinders transmission of the stress wave through the hard rock and entraps most energy into the concrete slab. The back-calculated concrete thickness matches well with the real thickness, which confirms numerical stability.
- A train load module is developed by converting the train load into time-variant equivalent forces based on the shape functions. The applied concentrated load traveling along the beam node induces a general stress distribution below the sleeper in time, which validates the implementation of the moving load.
- The fully bonded and void condition states are simulated with two train classes. The time domain waveforms show the number of peak accelerations associated with the train class and the moving time along the beam nodes. Compared to the fully bonded state, the presence of a void condition amplifies the acceleration and vibration response.
- The STFT analysis highlights that the void condition increases the energy density and the contour shape is stretched parallel to the frequency axis at around 120 Hz.

Acknowledgments

This research was supported by the “Development of key subsea tunneling technology” program (16SCIPB066321-03) funded by the Korea Agency for Infrastructure Technology Advancement (KAIA).

References

- ABAQUS (2011), ABAQUS Documentation; Dassault Systèmes, Providence, RI, USA.
- Bian, X., Jiang, H., Chang, C., Hu, J. and Chen, Y. (2015), “Track and ground vibrations generated by high-speed train running on ballastless railway with excitation of vertical track irregularities”, *Soil Dyn. Earthq. Eng.*, **76**, 29-43.
- Bian, X., Cheng, C., Jiang, J., Chen, R. and Chen, Y. (2016), “Numerical analysis of soil vibrations due to trains moving at critical speed”, *Acta Geotech.*, **11**(2), 281-294.
- Cai, Z. and Raymond, G.P. (1994), “Modelling the dynamic response of railway track to wheel/rail impact loading”, *Struct. Eng. Mech., Int. J.*, **2**(1), 95-112.
- Carino, N.J. (2013), “Training: Often the missing link in using NDT methods”, *Constr. Build. Mater.*, **38**, 1316-1329.
- Carino, N. and Sansalone, M. (1990), “Flaw Detection in Concrete Using the Impact-Echo Method”, In: *Bridge Evaluation, Repair and Rehabilitation*, (A. Nowak Ed.), Springer, Netherlands, pp. 101-118.
- Dawn, T.M. (1983), “Ground vibrations from heavy freight trains”, *J. Sound Vib.*, **87**(2), 351-356.
- De Chiara, F., Pereira, D., Fontul, S. and Fortunato, E. (2012), “Track Substructure Assessment using Non-

- Destructive Load Tests. A Portuguese Case Study”, *Procedia - Social and Behavioral Sciences*, **53**, 1129-1138.
- Gibson, A. and Popovics, J.S. (2005), “Lamb wave basis for impact-echo method analysis”, *J. Eng. Mech.*, **131**(4), 438-443.
- Hall, L. (2003), “Simulations and analyses of train-induced ground vibrations in finite element models”, *Soil Dyn. Earthq. Eng.*, **23**(5), 403-413.
- Hino, J., Yoshimura, T., Konishi, K. and Ananthanarayana, N. (1984), “A finite element method prediction of the vibration of a bridge subjected to a moving vehicle load”, *J. Sound Vib.*, **96**(1), 45-53.
- Hugenschmidt, J. (2000), “Railway track inspection using GPR”, *Journal of Applied Geophysics*, **43**(2-4), 147-155.
- Jiang, H., Bian, X., Cheng, C., Chen, Y. and Chen, R. (2016), “Simulating train moving loads in physical model testing of railway infrastructure and its numerical calibration”, *Acta Geotech.*, **11**(2), 231-242.
- Kouroussis, G., Connolly, D.P., Forde, M. and Verlinden, O. (2013a), “Train speed calculation using ground vibrations”, *Proceedings of the Institution of Mechanical Engineers, Part F: Journal of Rail and Rapid Transit*, **229**(5), 466-483.
- Kouroussis, G., Conti, C. and Verlinden, O. (2013b), “Investigating the influence of soil properties on railway traffic vibration using a numerical model”, *Vehicle Syst. Dyn.*, **51**(3), 421-442.
- Kouroussis, G., Connolly, D.P. and Verlinden, O. (2014), “Railway-induced ground vibrations – a review of vehicle effects”, *Int. J. Rail Transport.*, **2**(2), 69-110.
- KRRI (2006), Study on dynamic stability of railway subbase installed reinforcement; Korea Railroad Research Institute. [In Korean]
- Krylov, V.V. (1995), “Generation of ground vibrations by superfast trains”, *Appl. Acoust.*, **44**(2), 149-164.
- Lin, Y., Sansalone, M. and Carino, N. (1990), “Finite element studies of the impact-echo response of plates containing thin layers and voids”, *J. Nondestruct. Eval.*, **9**(1), 27-47.
- Lin, Y., Sansalone, M. and Carino, N.J. (1991), “Impact-echo response of concrete shafts”, *Geotech. Test. J.*, **14**(2), 121-137.
- Luo, X., Haya, H., Inaba, T., Shiotani, T. and Nakanishi, Y. (2004), “Damage evaluation of railway structures by using train-induced AE”, *Constr. Build. Mater.*, **18**(3), 215-223.
- Madshus, C. and Kaynia, A.M. (2000), “High-speed railway lines on soft ground: dynamic behaviour at critical train speed”, *J. Sound Vib.*, **231**(3), 689-701.
- Michaltsos, G., Sophianopoulos, D. and Kounadis, A.N. (1996), “The effect of a moving mass and other parameters on the dynamic response of a simply supported beam”, *J. Sound Vib.*, **191**(3), 357-362.
- Mosayebia, S.-A., Zakerib, J.-A. and Esmaili, M. (2017), “Vehicle/track dynamic interaction considering developed railway substructure models”, *Struct. Eng. Mech., Int. J.*, **61**(6), 775-784.
- Priest, J.A. and Powrie, W. (2009), “Determination of Dynamic Track Modulus from Measurement of Track Velocity during Train Passage”, *J. Geotech. Geoenviron. Eng.*, **135**(11), 1732-1740.
- Santamarina, J.C. and Fratta, D. (2005), *Discrete Signals and Inverse Problems: An Introduction for Engineers and Scientists*, ASCE Press.
- Song, K.-I. and Cho, G.-C. (2009), “Bonding state evaluation of tunnel shotcrete applied onto hard rocks using the impact-echo method”, *NDT & E International*, **42**(6), 487-500.
- Song, K.-I. and Cho, G.-C. (2010), “Numerical study on the evaluation of tunnel shotcrete using the Impact-Echo method coupled with Fourier transform and short-time Fourier transform”, *Int. J. Rock Mech. Mining Sci.*, **47**(8), 1274-1288.
- Sun, Q.D., Indraratna, B. and Nimbalkar, S. (2016), “Deformation and degradation mechanisms of railway ballast under high frequency cyclic loading”, *J. Geotech. Geoenviron. Eng.*, **142**(1), 04015056.
- Takemiya, H. and Bian, X. (2005), “Substructure simulation of inhomogeneous track and layered ground dynamic interaction under train passage”, *J. Eng. Mech.*, **131**(7), 699-711.
- Wu, J.-J., Whittaker, A.R. and Cartmell, M.P. (2000), “The use of finite element techniques for calculating the dynamic response of structures to moving loads”, *Comput. Struct.*, **78**(6), 789-799.